

CONTENTS

	Page
Acknowledgement	d
Abstract in Thai	e
Abstract in English	h
List of Tables	m
List of Figures	v
List of Abbreviations	dd
List of Symbols	ee
Statements of Originality in Thai	ff
Statements of Originality in English	gg
Chapter 1 Introduction	1
1.1 Background and motivation	1
1.2 Literature reviews	2
1.3 Purpose of the study	10
1.4 Research rationale	10
1.5 Educational advantages	10
1.6 Scope of the study	11
1.7 Research methodology	11
Chapter 2 Principles and Theories of the Study	12
2.1 Fuzzy set theory	12
2.2 Fuzzy clustering	14
2.2.1 The data set	15
2.2.2 Cluster prototypes	15
2.2.3 Fuzzy partition	15
2.2.4 The Fuzzy C-Means (FCM) clustering	16
2.3 Gray Level Co-occurrence Matrix (GLCM)	17
2.4 Multi-class Support Vector Machine (MSVM)	19

Chapter 3 System Design and Methodology	21
3.1 Fuzzy co-occurrence matrix texture descriptor	21
3.2 Fuzzy co-occurrence matrix properties	23
3.3 Fuzzy co-occurrence matrix texture features	24
Chapter 4 Gray Level Texture Classification Results and Discussions	28
4.1 Experimental design	28
4.2 Classification results and discussions	29
4.3 Summary	84
Chapter 5 Examination Mammogram Images using FCOM texture features	88
5.1 Experimental design	88
5.2 Detection results and discussions	90
5.3 Summary	107
Chapter 6 SAR Automatic Target Recognition using FCOM texture features	108
6.1 Experimental design	108
6.2 Recognition results and discussions	110
6.3 Summary	126
Chapter 7 Color Texture Classification Results and Discussions	131
7.1 Experimental design	131
7.2 Classification results and discussions	137
7.3 Summary	152
Chapter 8 Conclusion	154
References	158
List of Publication	166
Curriculum Vitae	167

LIST OF TABLES

	Page
Table 1.1 The summarized of literature reviews based on fuzzy set theory	10
Table 2.1 An example of SVM kernels	19
Table 4.1 A comparison of the textural feature sets	29
Table 4.2 The summarized results for the best correct classification from the Brodatz validation set where $d = 1$	41
Table 4.3 The summarized results for the best correct classification from the Brodatz validation set where $d = 2$	41
Table 4.4 The summarized results for the best correct classification from the Brodatz validation set where $d = 3$	41
Table 4.5 The summarized results for the best correct classification from the Brodatz validation set where $d = 4$	42
Table 4.6 The summarized results for the best correct classification from the Brodatz validation set where $d = 5$	42
Table 4.7 The summarized results for the best correct classification from the Brodatz validation set	42
Table 4.8 The summarized results for the best correct classification from the Kylberg validation set where $d = 1$	54
Table 4.9 The summarized results for the best correct classification from the Kylberg validation set where $d = 2$	54
Table 4.10 The summarized results for the best correct classification from the Kylberg validation set where $d = 3$	54
Table 4.11 The summarized results for the best correct classification from the Kylberg validation set where $d = 4$	55
Table 4.12 The summarized results for the best correct classification from the Kylberg validation set where $d = 5$	55
Table 4.13 The summarized results for the best correct classification from the Kylberg validation set	55

Table 4.14	The summarized results for the best correct classification from the UIUC validation set where $d = 1$	69
Table 4.15	The summarized results for the best correct classification from the UIUC validation set where $d = 2$	69
Table 4.16	The summarized results for the best correct classification from the UIUC validation set where $d = 3$	70
Table 4.17	The summarized results for the best correct classification from the UIUC validation set where $d = 4$	70
Table 4.18	The summarized results for the best correct classification from the UIUC validation set where $d = 5$	70
Table 4.19	The summarized results for the best correct classification from the UIUC validation set	71
Table 4.20	The summarized results for the best correct classification from the UMD validation set where $d = 1$	82
Table 4.21	The summarized results for the best correct classification from the UMD validation set where $d = 2$	82
Table 4.22	The summarized results for the best correct classification from the UMD validation set where $d = 3$	83
Table 4.23	The summarized results for the best correct classification from the UMD validation set where $d = 4$	83
Table 4.24	The summarized results for the best correct classification from the UMD validation set where $d = 5$	83
Table 4.25	The summarized results for the best correct classification from the UMD validation set	84
Table 4.26	The summary of the best gray scale validation set correct classification results	84
Table 5.1	The mammogram image textural feature sets comparison	89
Table 5.2	Summary of mammogram images data set	91
Table 5.3	The best validation set detection results from FCOM feature sets	92
Table 5.4	The best validation set detection result confusion matrices from FzCM1 at $C = 4$	92

Table 5.5	The best validation set detection result confusion matrices from FzCM2 at $C = 4$	92
Table 5.6	The best validation set detection result confusion matrices from FzCM3 at $C = 4$	93
Table 5.7	The best validation set detection result confusion matrices from FzCM4 at $C = 4$	93
Table 5.8	The best validation set detection result confusion matrices from FzCM5 at $C = 4$	93
Table 5.9	The best validation set detection result confusion matrices from FzCM6 at $C = 4$	93
Table 5.10	The best validation set detection result confusion matrices from FzCM1 at $C = 8$	94
Table 5.11	The best validation set detection result confusion matrices from FzCM2 at $C = 8$	94
Table 5.12	The best validation set detection result confusion matrices from FzCM3 at $C = 8$	94
Table 5.13	The best validation set detection result confusion matrices from FzCM4 at $C = 8$	94
Table 5.14	The best validation set detection result confusion matrices from FzCM5 at $C = 8$	95
Table 5.15	The best validation set detection result confusion matrices from FzCM6 at $C = 8$	95
Table 5.16	The best validation set detection results from GLCM feature sets	95
Table 5.17	The best validation set detection result confusion matrices from GLCM1 at $C = 4$	96
Table 5.18	The best validation set detection result confusion matrices from GLCM 2 at $C = 4$	96
Table 5.19	The best validation set detection result confusion matrices from GLCM 3 at $C = 4$	96
Table 5.20	The best validation set detection result confusion matrices from GLCM 4 at $C = 4$	96

Table 5.21	The best validation set detection result confusion matrices from GLCM 5 at $C = 4$	97
Table 5.22	The best validation set detection result confusion matrices from GLCM 6 at $C = 4$	97
Table 5.23	The best validation set detection result confusion matrices from GLCM 1 at $C = 8$	97
Table 5.24	The best validation set detection result confusion matrices from GLCM 2 at $C = 8$	97
Table 5.25	The best validation set detection result confusion matrices from GLCM 3 at $C = 8$	98
Table 5.26	The best validation set detection result confusion matrices from GLCM 4 at $C = 8$	98
Table 5.27	The best validation set detection result confusion matrices from GLCM 5 at $C = 8$	98
Table 5.28	The best validation set detection result confusion matrices from GLCM 6 at $C = 8$	98
Table 5.29	The best detection result on blind test data set.	101
Table 5.30	The detection result details from FzCM3 at $C = 8$	102
Table 5.31	The detection result details from FzCM2 at $C = 4$	102
Table 5.32	The detection result details from GLCM2 at $N_g = 8$	103
Table 5.33	The detection result details from GLCM6 at $N_g = 8$	104
Table 6.1	FCOM and GLCM feature sets	109
Table 6.2	Dimensions of FCOM feature sets	110
Table 6.3	MSTAR data set	111
Table 6.4	Examples of SAR image objects in different window sizes	111
Table 6.5	The best classification rates using FCOM for $d = 1, 2, 3, 5,$ and 10	112
Table 6.6	Confusion matrices of the results in table 6.5 from MSVM for $d = 1$	112
Table 6.7	Confusion matrices of the results in table 6.5 from MSVM for $d = 2$	112
Table 6.8	Confusion matrices of the results in table 6.5 from MSVM for $d = 3$	113
Table 6.9	Confusion matrices of the results in table 6.5 from MSVM for $d = 5$	113
Table 6.10	Confusion matrices of the results in table 6.5 from MSVM for $d = 10$	113

Table 6.11	Confusion matrices of the results in table 6.5 from RBF network for $d = 1$	113
Table 6.12	Confusion matrices of the results in table 6.5 from RBF network for $d = 2$	113
Table 6.13	Confusion matrices of the results in table 6.5 from RBF network for $d = 3$	114
Table 6.14	Confusion matrices of the results in table 6.5 from RBF network for $d = 5$	114
Table 6.15	Confusion matrices of the results in table 6.5 from RBF network for $d = 10$	114
Table 6.16	The best classification rates using GLCM for $d = 1, 2, 3, 5,$ and 10	115
Table 6.17	Confusion matrices of the results in table 6.16 from MSVM for $d = 1$	115
Table 6.18	Confusion matrices of the results in table 6.16 from MSVM for $d = 2$	115
Table 6.19	Confusion matrices of the results in table 6.16 from MSVM for $d = 3$	116
Table 6.20	Confusion matrices of the results in table 6.16 from MSVM for $d = 5$	116
Table 6.21	Confusion matrices of the results in table 6.16 from MSVM for $d = 10$	116
Table 6.22	Confusion matrices of the results in table 6.16 from RBF network $d = 1$	116
Table 6.23	Confusion matrices of the results in table 6.16 from RBF network $d = 2$	116
Table 6.24	Confusion matrices of the results in table 6.16 from RBF network $d = 3$	117
Table 6.25	Confusion matrices of the results in table 6.16 from RBF network $d = 5$	117
Table 6.26	Confusion matrices of the results in table 6.16 from RBF network $d = 10$	117
Table 6.27	Ensemble average fusion results from the 10 best models using FCOM at $d = 1, 2, 3, 5,$ and 10	118
Table 6.28	Confusion matrices of the results in table 6.27 for $d = 1$	118

Table 6.29	Confusion matrices of the results in table 6.27 for $d = 2$	118
Table 6.30	Confusion matrices of the results in table 6.27 for $d = 3$	118
Table 6.31	Confusion matrices of the results in table 6.27 for $d = 5$	118
Table 6.32	Confusion matrices of the results in table 6.27 for $d = 10$	119
Table 6.33	Ensemble average fusion results from the 10 best models using GLCM at $d = 1, 2, 3, 5,$ and 10	119
Table 6.34	Confusion matrices of the results in table 6.33 for $d = 1$	119
Table 6.35	Confusion matrices of the results in table 6.33 for $d = 2$	119
Table 6.36	Confusion matrices of the results in table 6.33 for $d = 3$	120
Table 6.37	Confusion matrices of the results in table 6.33 for $d = 5$	120
Table 6.38	Confusion matrices of the results in table 6.33 for $d = 10$	120
Table 6.39	Ensemble average fusion results from the M best models using FCOM at different feature sets, different d , different N , and different σ	121
Table 6.40	Confusion matrices of the best results in table 6.39 for $d = 1, 2, 3, 5,$ and 10	121
Table 6.41	Confusion matrices of the best results in table 6.39 for $d = 2, 3, 5,$ and 10	122
Table 6.42	Confusion matrices of the best results in table 6.39 for $d = 3, 5,$ and 10	122
Table 6.43	Confusion matrices of the best results in table 6.39 for $d = 5$ and 10	122
Table 6.44	Ensemble average fusion results from the M best models using GLCM at different feature sets, different d , different N , and different σ	122
Table 6.45	Confusion matrices of the best results in table 6.44 for $d = 1, 2, 3, 5,$ and 10	123
Table 6.46	Confusion matrices of the best results in table 6.44 for $d = 2, 3, 5,$ and 10	123

Table 6.47	Confusion matrices of the best results in table 6.44 for $d = 3, 5,$ and 10	123
Table 6.48	Confusion matrices of the best results in table 6.44 for $d = 5$ and 10	123
Table 6.49	MSVM and RBF network ensemble average fusion results from the M best models at different feature sets, different d , different N , and different σ	124
Table 6.50	Confusion matrices of the best results in table 6.49 for $d = 1, 2, 3, 5,$ and 10	125
Table 6.51	Confusion matrices of the best results in table 6.49 for $d = 2, 3, 5,$ and 10	125
Table 6.52	Confusion matrices of the best results in table 6.49 for $d = 3, 5,$ and 10	125
Table 6.53	Confusion matrices of the best results in table 6.49 for $d = 5$ and 10	125
Table 6.54	Summarized of the best MSTAR SAR detection results	126
Table 7.1	The color feature sets comparison	134
Table 7.2	Summary of color texture data sets	135
Table 7.3	The best correct classification results from GLCM on the Outex validation set	136
Table 7.4	The best correct classification result from FCOM on the Outex validation set	137
Table 7.5	The best correct classification result from FCLCOM on the Outex validation set	137
Table 7.6	The best correct classification result from CLCM on the Outex validation set	137
Table 7.7	The summary of the best validation set classification results on the Outex data set	138
Table 7.8	The best correct classification result from GLCM on the USPTex validation set	140

Table 7.9	The best correct classification result from FCOM on the USPTex validation set	141
Table 7.10	The best correct classification result from FCLCOM on the USPTex validation set	141
Table 7.11	The best correct classification result from CLCM on the USPTex validation set	141
Table 7.12	The summary of best validation set classification results on the USPTex data set	142
Table 7.13	The best correct classification result from GLCM on the Biomass validation set	145
Table 7.14	The best correct classification result from FCOM on the Biomass validation set	145
Table 7.15	The best correct classification result from FCLCOM on the Biomass validation set	146
Table 7.16	The best correct classification result from CLCM on the Biomass validation set	146
Table 7.17	The summary of the best validation set classification results on the Biomass data set	146
Table 7.18	The best correct classification result from GLCM on the MondialMarmi validation set	148
Table 7.19	The best correct classification result from FCOM on the MondialMarmi validation set	148
Table 7.20	The best correct classification result from FCLCOM on the MondialMarmi validation set	149
Table 7.21	The best correct classification result from CLCM on the MondialMarmi validation set	149
Table 7.22	The summary of best validation set classification results on the MondialMarmi data set	149
Table 7.23	The best correct classification result from GLCM on the NewBarkTex validation set	151
Table 7.24	The best correct classification result from FCOM on the NewBarkTex validation set	151

Table 7.25	The best correct classification result from FCLCOM on the NewBarkTex validation set	151
Table 7.26	The best correct classification result from CLCM on the NewBarkTex validation set	152
Table 7.27	The summary of the best validation set classification results on the NewBarkTex data set	152
Table 7.28	The summary of the best validation color texture classification results	153



ลิขสิทธิ์มหาวิทยาลัยเชียงใหม่
 Copyright© by Chiang Mai University
 All rights reserved

LIST OF FIGURES

	Page
Figure 1.1 An example of textures in human observation	2
Figure 1.2 An example of textures in computer vision	2
Figure 1.3 An example of textures in mathematical perspective	2
Figure 2.1 The GLCM orientation assignment	18
Figure 2.2 An example of discriminative hyperplanes	19
Figure 3.1 The fuzzy co-occurrence matrix texture feature extraction workflow	21
Figure 3.2 An example of the fuzzy co-occurrence matrix construction	23
Figure 4.1 An example of Brodatz texture data set	30
Figure 4.2 The best validation set classification results from the Brodatz data set where N_g or $C = 4$ and $d = 1$	31
Figure 4.3 The best validation set classification results from the Brodatz data set where N_g or $C = 4$ and $d = 2$	31
Figure 4.4 The best validation set classification results from the Brodatz data set where N_g or $C = 4$ and $d = 3$	32
Figure 4.5 The best validation set classification results from the Brodatz data set where N_g or $C = 4$ and $d = 4$	32
Figure 4.6 The best validation set classification results from the Brodatz data set where N_g or $C = 4$ and $d = 5$	33
Figure 4.7 The best validation set classification results from the Brodatz data set where N_g or $C = 8$ and $d = 1$	33
Figure 4.8 The best validation set classification results from the Brodatz data set where N_g or $C = 8$ and $d = 2$	34
Figure 4.9 The best validation set classification results from the Brodatz data set where N_g or $C = 8$ and $d = 3$	34
Figure 4.10 The best validation set classification results from the Brodatz data set where N_g or $C = 8$ and $d = 4$	35
Figure 4.11 The best validation set classification results from the Brodatz data set where N_g or $C = 8$ and $d = 5$	35

Figure 4.12	The best validation set classification results from the Brodatz data set where N_g or $C = 16$ and $d = 1$	36
Figure 4.13	The best validation set classification results from the Brodatz data set where N_g or $C = 16$ and $d = 2$	36
Figure 4.14	The best validation set classification results from the Brodatz data set where N_g or $C = 16$ and $d = 3$	37
Figure 4.15	The best validation set classification results from the Brodatz data set where N_g or $C = 16$ and $d = 4$	37
Figure 4.16	The best validation set classification results from the Brodatz data set where N_g or $C = 16$ and $d = 5$	38
Figure 4.17	The best validation set classification results from the Brodatz data set where N_g or $C = 32$ and $d = 1$	38
Figure 4.18	The best validation set classification results from the Brodatz data set where N_g or $C = 32$ and $d = 2$	39
Figure 4.19	The best validation set classification results from the Brodatz data set where N_g or $C = 32$ and $d = 3$	39
Figure 4.20	The best validation set classification results from the Brodatz data set where N_g or $C = 32$ and $d = 4$	40
Figure 4.21	The best validation set classification results from the Brodatz data set where N_g or $C = 32$ and $d = 5$	40
Figure 4.22	An example of Kylbert texture data set	43
Figure 4.23	The best validation set classification results from the Kylberg data set where N_g or $C = 4$ and $d = 1$	44
Figure 4.24	The best validation set classification results from the Kylberg data set where N_g or $C = 4$ and $d = 2$	44
Figure 4.25	The best validation set classification results from the Kylberg data set where N_g or $C = 4$ and $d = 3$	45
Figure 4.26	The best validation set classification results from the Kylberg data set where N_g or $C = 4$ and $d = 4$	45
Figure 4.27	The best validation set classification results from the Kylberg data set where N_g or $C = 4$ and $d = 5$	46

Figure 4.28 The best validation set classification results from the Kylberg data set where N_g or $C = 8$ and $d = 1$	46
Figure 4.29 The best validation set classification results from the Kylberg data set where N_g or $C = 8$ and $d = 2$	47
Figure 4.30 The best validation set classification results from the Kylberg data set where N_g or $C = 8$ and $d = 3$	47
Figure 4.31 The best validation set classification results from the Kylberg data set where N_g or $C = 8$ and $d = 4$	48
Figure 4.32 The best validation set classification results from the Kylberg data set where N_g or $C = 8$ and $d = 5$	48
Figure 4.33 The best validation set classification results from the Kylberg data set where N_g or $C = 16$ and $d = 1$	49
Figure 4.34 The best validation set classification results from the Kylberg data set where N_g or $C = 16$ and $d = 2$	49
Figure 4.35 The best validation set classification results from the Kylberg data set where N_g or $C = 16$ and $d = 3$	50
Figure 4.36 The best validation set classification results from the Kylberg data set where N_g or $C = 16$ and $d = 4$	50
Figure 4.37 The best validation set classification results from the Kylberg data set where N_g or $C = 16$ and $d = 5$	51
Figure 4.38 The best validation set classification results from the Kylberg data set where N_g or $C = 32$ and $d = 1$	51
Figure 4.39 The best validation set classification results from the Kylberg data set where N_g or $C = 32$ and $d = 2$	52
Figure 4.40 The best validation set classification results from the Kylberg data set where N_g or $C = 32$ and $d = 3$	52
Figure 4.41 The best validation set classification results from the Kylberg data set where N_g or $C = 32$ and $d = 4$	53
Figure 4.42 The best validation set classification results from the Kylberg data set where N_g or $C = 32$ and $d = 5$	53
Figure 4.43 An example of incorrect classification image on Kylberg data set	56
Figure 4.44 Vertical texture and corresponding GLCM and FCOM planes	57

Figure 4.45 Horizontal texture and corresponding GLCM and FCOM planes	58
Figure 4.46 Regular texture and corresponding GLCM and FCOM planes	58
Figure 4.47 An example of UIUC texture data set	59
Figure 4.48 The best validation set classification results from the UIUC data set where N_g or $C = 4$ and $d = 1$	59
Figure 4.49 The best validation set classification results from the UIUC data set where N_g or $C = 4$ and $d = 2$	60
Figure 4.50 The best validation set classification results from the UIUC data set where N_g or $C = 4$ and $d = 3$	60
Figure 4.51 The best validation set classification results from the UIUC data set where N_g or $C = 4$ and $d = 4$	61
Figure 4.52 The best validation set classification results from the UIUC data set where N_g or $C = 4$ and $d = 5$	61
Figure 4.53 The best validation set classification results from the UIUC data set where N_g or $C = 8$ and $d = 1$	62
Figure 4.54 The best validation set classification results from the UIUC data set where N_g or $C = 8$ and $d = 2$	62
Figure 4.55 The best validation set classification results from the UIUC data set where N_g or $C = 8$ and $d = 3$	63
Figure 4.56 The best validation set classification results from the UIUC data set where N_g or $C = 8$ and $d = 4$	63
Figure 4.57 The best validation set classification results from the UIUC data set where N_g or $C = 8$ and $d = 5$	64
Figure 4.58 The best validation set classification results from the UIUC data set where N_g or $C = 16$ and $d = 1$	64
Figure 4.59 The best validation set classification results from the UIUC data set where N_g or $C = 16$ and $d = 2$	65
Figure 4.60 The best validation set classification results from the UIUC data set where N_g or $C = 16$ and $d = 3$	65
Figure 4.61 The best validation set classification results from the UIUC data set where N_g or $C = 16$ and $d = 4$	66

Figure 4.62 The best validation set classification results from the UIUC data set where N_g or $C = 16$ and $d = 5$	66
Figure 4.63 The best validation set classification results from the UIUC data set where N_g or $C = 32$ and $d = 1$	67
Figure 4.64 The best validation set classification results from the UIUC data set where N_g or $C = 32$ and $d = 2$	67
Figure 4.65 The best validation set classification results from the UIUC data set where N_g or $C = 32$ and $d = 3$	68
Figure 4.66 The best validation set classification results from the UIUC data set where N_g or $C = 32$ and $d = 4$	68
Figure 4.67 The best validation set classification results from the UIUC data set where N_g or $C = 32$ and $d = 5$	69
Figure 4.68 Example of incorrect classification images on UIUC data set	70
Figure 4.69 An example of UMD texture data set	72
Figure 4.70 The best validation set classification results from the UMD data set where N_g or $C = 4$ and $d = 1$	72
Figure 4.71 The best validation set classification results from the UMD data set where N_g or $C = 4$ and $d = 2$	73
Figure 4.72 The best validation set classification results from the UMD data set where N_g or $C = 4$ and $d = 3$	73
Figure 4.73 The best validation set classification results from the UMD data set where N_g or $C = 4$ and $d = 4$	74
Figure 4.74 The best validation set classification results from the UMD data set where N_g or $C = 4$ and $d = 5$	74
Figure 4.75 The best validation set classification results from the UMD data set where N_g or $C = 8$ and $d = 1$	75
Figure 4.76 The best validation set classification results from the UMD data set where N_g or $C = 8$ and $d = 2$	75
Figure 4.77 The best validation set classification results from the UMD data set where N_g or $C = 8$ and $d = 3$	76
Figure 4.78 The best validation set classification results from the UMD data set where N_g or $C = 8$ and $d = 4$	76

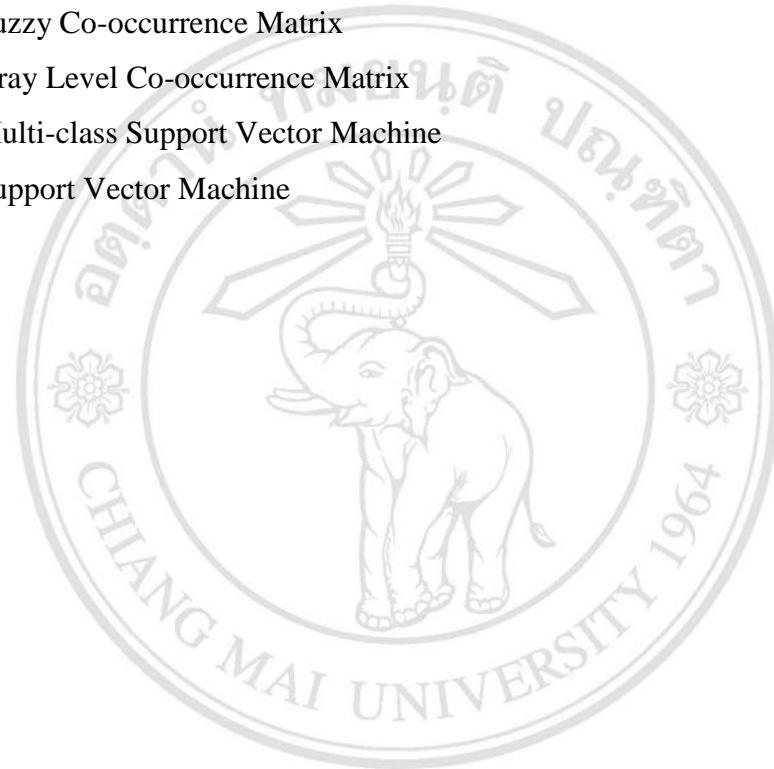
Figure 4.79 The best validation set classification results from the UMD data set where N_g or $C = 8$ and $d = 5$	77
Figure 4.80 The best validation set classification results from the UMD data set where N_g or $C = 16$ and $d = 1$	77
Figure 4.81 The best validation set classification results from the UMD data set where N_g or $C = 16$ and $d = 2$	78
Figure 4.82 The best validation set classification results from the UMD data set where N_g or $C = 16$ and $d = 3$	78
Figure 4.83 The best validation set classification results from the UMD data set where N_g or $C = 16$ and $d = 4$	79
Figure 4.84 The best validation set classification results from the UMD data set where N_g or $C = 16$ and $d = 5$	79
Figure 4.85 The best validation set classification results from the UMD data set where N_g or $C = 32$ and $d = 1$	80
Figure 4.86 The best validation set classification results from the UMD data set where N_g or $C = 32$ and $d = 2$	80
Figure 4.87 The best validation set classification results from the UMD data set where N_g or $C = 32$ and $d = 3$	81
Figure 4.88 The best validation set classification results from the UMD data set where N_g or $C = 32$ and $d = 4$	81
Figure 4.89 The best validation set classification results from the UMD data set where N_g or $C = 32$ and $d = 5$	82
Figure 4.90 Example of incorrect classification images on UMD data set	84
Figure 4.91 Examples of difference brightness images and corresponding quantized images from GLCM and FCOM	86
Figure 4.92 Corresponding GLCM where $N_g = 8$ for image in figure 4.91	86
Figure 4.93 Corresponding FCOM where $C = 8$ for image in figure 4.91	86
Figure 5.1 Abnormalities mammogram image detection system	90
Figure 5.2 An example of sub-images in the signature library	91
Figure 5.3 Example results of ARCH detection from FzCM4 at $C = 4$	99
Figure 5.4 Example results of SPIC detection from FzCM4 at $C = 4$	100
Figure 5.5 Example results of CALC detection from FzCM4 at $C = 4$	100

Figure 5.6	Example results of CIRC detection from FzCM4 at $C = 4$	101
Figure 5.7	Example of CALC area (in black circle) that is overlapped with SPIC (in white circle)	105
Figure 5.8	Example of SPIC (MDB190) area without spike	105
Figure 5.9	Results of SPIC detection from MDB190	105
Figure 5.10	Example of CIRC area that is misclassified	106
Figure 5.11	An example for each class of abnormality types that least detected	106
Figure 5.12	An example of most created false alarm images	107
Figure 6.1	System workflow for SAR automatic target recognition	110
Figure 6.2	Classification results with different FCOM distance	112
Figure 6.3	Classification results with different GLCM distance	115
Figure 6.4	The first fusion scheme used in this experiment	116
Figure 6.5	The second fusion scheme used in this experiment	121
Figure 6.6	The third fusion scheme used in this experiment	124
Figure 6.7	(a) original BMP2 SAR image and (b) its corresponding sub-image ($N = 35$), the value of each FCOM planes for (c) $d = 1$, (d) $d = 2$, (e) $d = 3$, (f) $d = 5$, and (g) $d = 10$	128
Figure 6.8	GLCM and FCOM planes where $d = 10$ and $\theta = 0^\circ$ with different number of gray levels	129
Figure 6.9	Example of similar FCOM planes between different objects	130
Figure 7.1	FCLCOM extraction framework	133
Figure 7.2	CLCM orientation assignment	133
Figure 7.3	Color texture classification framework	134
Figure 7.4	An example of the Outex color texture data set	136
Figure 7.5	Incorrect classification images of the Outex from GLCM texture feature	138
Figure 7.6	Incorrect classification images of the Outex from CLCM texture feature	138
Figure 7.7	Incorrect classification images of the Outex from FCOM texture feature	139
Figure 7.8	Incorrect classification images of the Outex from FCLCOM texture feature	139

Figure 7.9	An example of the USPTex color texture data set	140
Figure 7.10	Incorrect classification images of the USPTex from GLCM texture feature	142
Figure 7.11	Incorrect classification images of the USPTex from CLCM texture feature	143
Figure 7.12	Incorrect classification images of the USPTex from FCOM texture feature	143
Figure 7.13	Incorrect classification images of the USPTex from FCLCOM texture feature	144
Figure 7.14	An example of the Biomass color texture data set	145
Figure 7.15	An example of the MondialMarmi color texture data set	148
Figure 7.16	An example of the NewBarkTex color texture data set	150

LIST OF ABBREVIATIONS

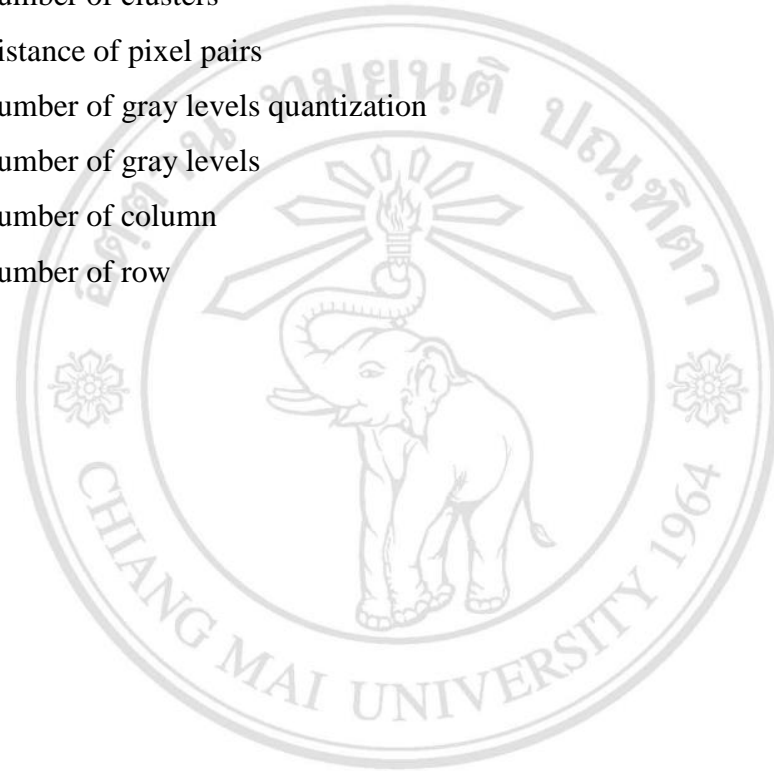
CLCM	Color Level Co-occurrence Matrix
FCLCOM	Fuzzy Color Level Co-occurrence Matrix
FCM	Fuzzy C-Means Clustering
FCOM	Fuzzy Co-occurrence Matrix
GLCM	Gray Level Co-occurrence Matrix
MSVM	Multi-class Support Vector Machine
SVM	Support Vector Machine



ลิขสิทธิ์มหาวิทยาลัยเชียงใหม่
Copyright© by Chiang Mai University
All rights reserved

LIST OF SYMBOLS

α	Alpha, Coefficient
Σ	Sigma, Summation
θ	Theta, Orientation Assignment
C	Number of clusters
d	Distance of pixel pairs
N_g	Number of gray levels quantization
N_l	Number of gray levels
N_x	Number of column
N_y	Number of row



ลิขสิทธิ์มหาวิทยาลัยเชียงใหม่
Copyright© by Chiang Mai University
All rights reserved

ข้อความแห่งการริเริ่ม

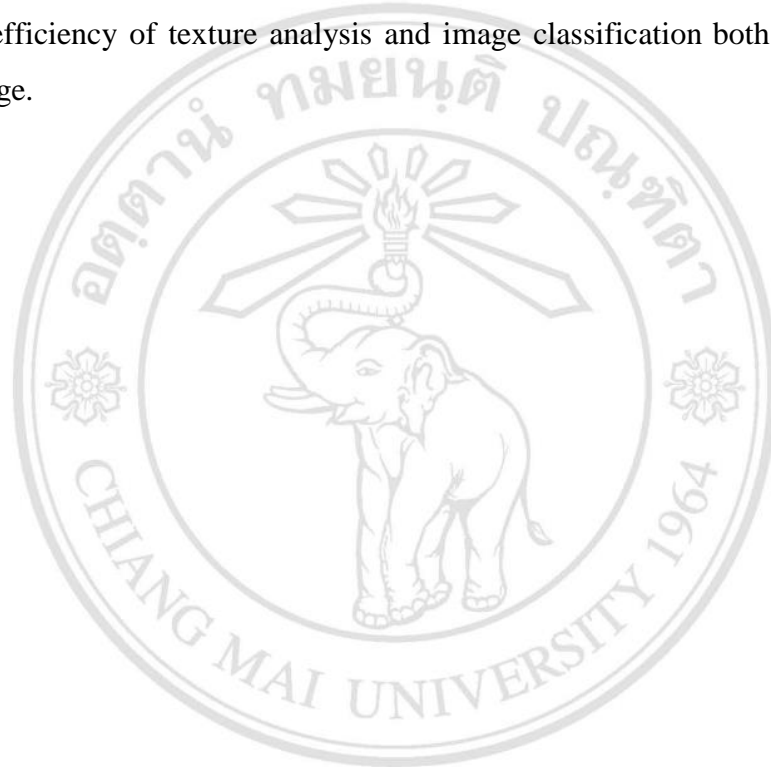
วิทยานิพนธ์นี้ได้นำเสนอวิธีการใหม่ในการสกัดลักษณะเด่นจากลักษณะของพื้นผิวสำหรับการวิเคราะห์และจำแนกรูปภาพ ที่อยู่บนพื้นฐานแนวความคิดของพีชซีเซต โดยอาศัยการผสมผสานการจัดกลุ่มแบบพีชซีเข้ากับเมทริกซ์ของการเกิดร่วมของระดับสีเทา วิธีการใหม่นี้สามารถเพิ่มประสิทธิภาพของการวิเคราะห์ลวดลายพื้นผิวและจำแนกรูปภาพทั้งที่เป็นภาพระดับสีเทาและภาพสีต่าง ๆ ได้ดีขึ้น



ลิขสิทธิ์มหาวิทยาลัยเชียงใหม่
Copyright© by Chiang Mai University
All rights reserved

STATEMENTS OF ORIGINALITY

This thesis proposes a new method of texture feature extraction for image analysis and classification based on fuzzy set theory. The method is developed by incorporating the fuzzy clustering into gray level co-occurrence matrix. The new method is able to improve the efficiency of texture analysis and image classification both of gray scale and color image.



ลิขสิทธิ์มหาวิทยาลัยเชียงใหม่
Copyright© by Chiang Mai University
All rights reserved